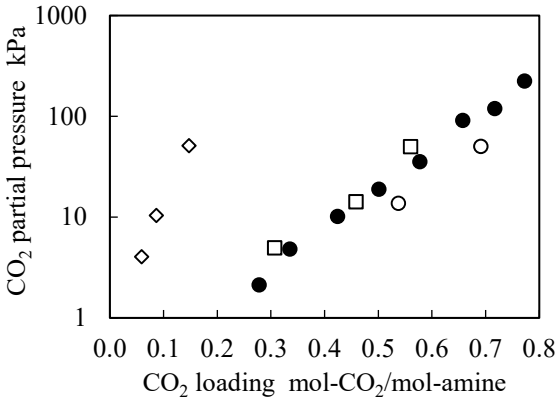

Figure 4. VLE curves of AMP 50wt%+MAPA 5wt% solution. ○, 50°C; □, 60°C; ◊, 120°C; and ●, Dash *et al*. (2011) AMP = 43wt% at 55°C

2.3 Measurement of precipitation and dissolution temperature

Precipitation and dissolution temperature of carbonate were measured by heating and cooling solution in a glass container to determine the precipitation boundary of AMP/MAPA solution selected as described in section 2.1. CO_2 loading of solution was 0.15–0.45 (mol-CO_2/mol-amine). Figure 5 shows the measurement result and the precipitation boundary against the temperature-dependent loading. Precipitation can be avoided by maintaining a temperature >60°C under a CO_2 partial pressure of 15 kPa.

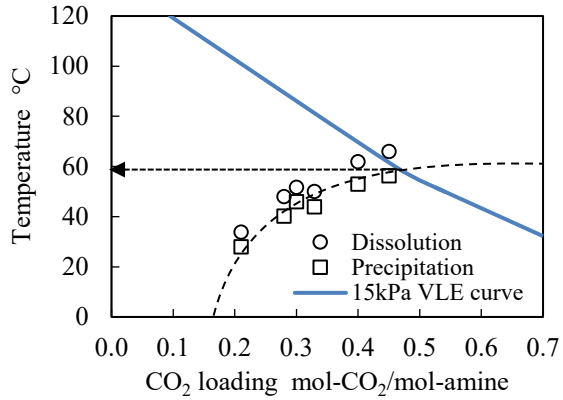

Figure 5. Boundary of precipitation against temperature and CO_2 loading. Blue line is VLE curve of CO_2 partial pressure 15kPa.

2.4 Cooling precipitation test

The cooling temperature required to induce carbonate precipitation was obtained by batch testing. The theoretical formula of Kubota (Kobari, 2014) is shown in Eq. (1), where ΔT_{ind} is the degree of supersaturation, $(N/M)_m$ is the assumed number density of primary nuclei for detection sensitivity k_{b1} is the primary nucleation constant, n is nucleation order, and ΔT is the degree of supercooling.

$$\log(\Delta T_{ind}) = \log[(N/M)_m / k_{b1}] - n\log(\Delta T) \quad (1)$$

Logarithmic plots of ΔT and lag time to precipitation are linear as shown in Eq. (1), and k_{b1} can be determined by the slope and intercept (isothermal method). After quenching 5 mL AMP 50 wt% solution, the temperature was held constant and the lag time to carbonate precipitation was measured. The primary nucleation constant was calculated from the measured time, the supersaturation degree, and the cooling temperature in the CO_2 capture and recovery test. The assumed number density of primary nuclei for detection sensitivity was set to $(N/M)_m$ = 500. Figure 6 shows the results of testing, which indicates the waiting time for precipitation against the degree of supersaturation become shorter as the CO_2 loading increase. Calculating k_{b1} and n in Eq. (1) by the plots and substituting waiting time of solution in cooling container into Eq. (1) gives the required degree of supersaturation for precipitation. The CO_2 loading in the bottom of absorber was assumed to be 0.45, and the waiting time of solution in cooling container was 2010 seconds, so the degree of supersaturation was determined to be 6.4°C (T = 53.6°C).

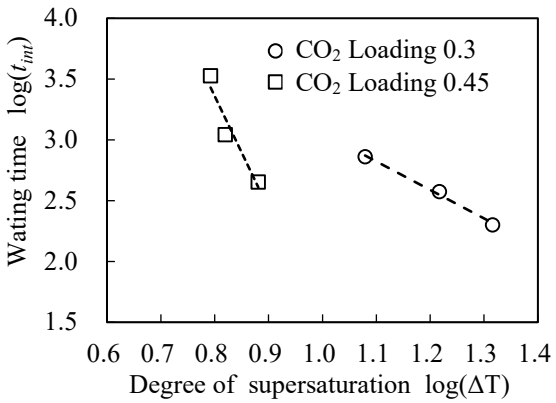

Figure 6. Waiting time for precipitation measured by isothermal method

2.5 Carbonate analysis

If MAPA is contained in the precipitates, then regeneration heat must be examined considering this MAPA-carbonate structure. Carbonate was analysed by Raman spectroscopy and gas chromatography and mass spectrometry (GC- MS) to confirm whether MAPA was contained in the precipitate. Figure. 7 shows the Raman spectra of the precipitates from AMP 50 wt%, AMP 50 wt%+MAPA 5 wt%, pure AMP, and pure MAPA. Although peaks commonly observed for hydrocarbons and AMP were detected in the spectrum for AMP+MAPA, no peaks specific to MAPA were not detected (see Figure 7).

Figure 8 shows the analysis results of AMP 50 wt%+MAPA 5 wt%, AMP 100%, and MAPA 100% by GC-MS. Spectra of pure AMP and AMP 50 wt%+MAPA 5 wt% were observed at an elapsed period of 6.6 minutes, the peak of pure MAPA was observed at a period of 7.4

minutes. According to the above result, the carbonate precipitated in AMP/ MAPA solution did not contain any salts derived from MAPA.

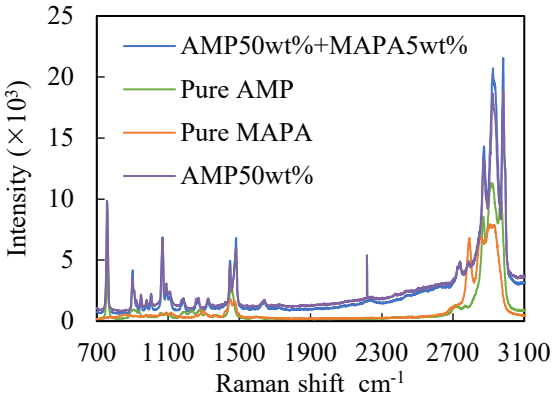

Figure 7. Raman spectra of the precipitates from the AMP 50 wt%+MAPA 5 wt%. For comparison, the spectra of pure AMP, pure MAPA, and the precipitates from AMP 50 wt% are also graphed.

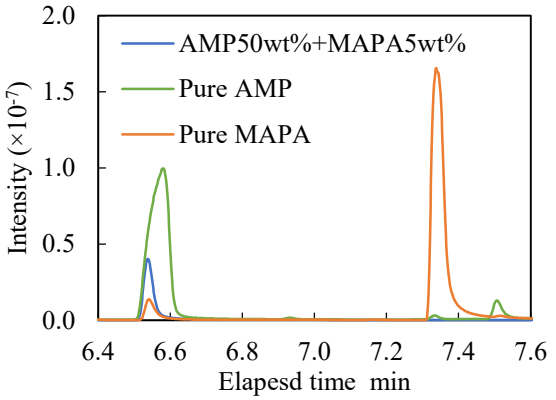

Figure 8. GC-MS spectra of precipitates from AMP 50wt%+MAPA 5wt% solution. Pure AMP and pure MAPA solution are graphed for comparison

3 Mid-column Injection Process

In our previous study of the phase separation process, separated CO_2 semi-lean liquid was mixed with CO_2 lean liquid and sent to the top of the absorber column. However, returning partially loaded solution (i.e., semi-lean liquid) to the top decreases the local absorption flux at the upper portion where is low CO_2 partial pressure. By injecting semi-lean liquid into the middle of the absorber column, the local CO_2 absorption driving force is maintained. This modification can improve the CO_2 absorption rate.

Figure 9 shows the partial model of the absorber built on the process simulator Aspen Plus®. The absorber column consisted of 10 stages. The change of CO_2 recovery rate and precipitate quantity was simulated when the injection stage was changed stepwise from Stage 1 (top) to Stage 10 (bottom). Figure 10 shows the calculation results of AMP 50wt% solution. The CO_2 recovery rate and the precipitate quantity peaked when semi-lean liquid was injected at Stage 5, equivalent to the central portion of the absorber column. From this test results, the injection position of semi-lean liquid was set to the middle of the absorber column.

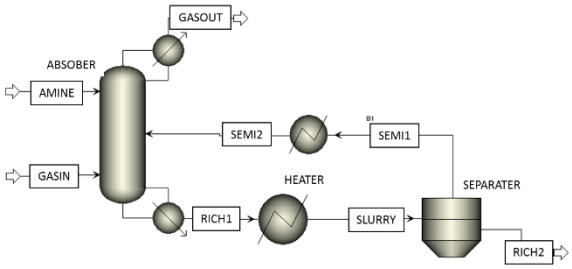

Figure 9. Partial model of absorber with variable injection location and precipitation of the CO_2-rich phase

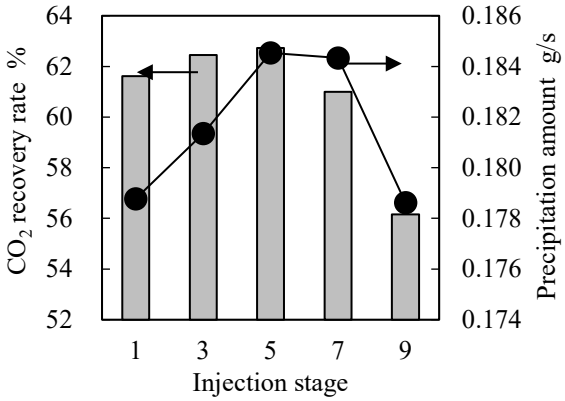

Figure 10. CO_2 recovery rate and precipitation amount at each injection stage

4 Evaluation by continuous CO_2 Capture and Recovery Test

4.1 Experimental apparatus

The new mixed amine and new injection location were evaluated by continuous CO_2 capture and recovery tests using the apparatus shown in Figure 11. The main points in the process are highlighted by numbers (1–5) and letters (S, L) in circles; these points correspond to Figure 1. The new injection location is designated by ①' in Figure 11.

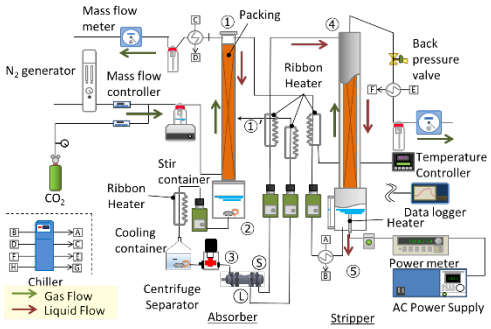

Figure 11. 10 kg/day-scale apparatus of CO_2 capture and recovery

The temperature in absorber must be maintained above the precipitation temperature to prevent passage blockage. To avoid precipitation prior to reaching the cooling container, the temperature of the lower of absorber and transfer lines to the cooling container were maintained at 65.0°C. The cooling container was chilled at the precipitation temperature of around 53.0˚C by 20.0°C brine with natural cooling without insulation.

The amine concentration in solution was reduced to 40 wt% in the CO_2 capture and recovery test because the amount of precipitate increases by lowering the amine concentration under the condition of a constant liquid gas ratio.

Table 1 shows this test conditions.

Table 1. Conditions of CO_2 recovery tests using AMP 50wt%+MAPA 5 wt%

Liquid gas ratio	6
CO_2 gas flow rate [L/min]	2.2
N_2 gas flow rate [L/min]	12.7
CO_2 partial pressure [kPa]	15
Upper stripper temperature [°C]	110
Lower stripper temperature [°C]	120
Electric power input of heater [W]	250

4.2 Operation stability

Operation stability of CO_2 capture and recovery test including continuous precipitation and centrifugal separation was checked by material balance of CO_2. Material balance of CO_2 can be evaluated by two way which are the CO_2 captured in the absorber, and CO_2 gas flow rate from the outlet of stripper, shown in Table 2. The difference between these flow rates was about 1.0%, and it was confirmed that the experiment was operated stably.

Table 2. CO_2 flow rate and difference between lean and rich loading of solution.

CO_2 captured in the absorber [g/h]	217
CO_2 gas flow rate from the outlet of stripper [g/h]	215

4.3 Regeneration heat and CO_2 recovery rate

Regeneration heat Q_{in} in this test was measured by electrical energy of the heater at the bottom of stripper compensating inherent heat loss of the stripper Q_{loss}. The CO_2 dissociation heat Q_R [GJ/ton-CO_2] was obtained by Eq. (2), where Q_V is the vaporization heat, Q_H is the sensible heat.

$$Q_R = Q_{in} - Q_V - Q_H - Q_{loss} \quad (2)$$

Q_V was obtained by Eq. (3), where the stripper vapor flow rate is given by W_V [kg/h], the latent heat is H_V [MJ/kg], and the recovery CO_2 flow rate is W_{CO2} [kg-CO_2/h].

$$Q_V = W_V H_V / W_{CO2} \quad (3)$$

The sensible heat was obtained by Eq. (4), where the liquid flow rate is W_S [kg/h], specific heat is C_p [MJ/kg/K], the stripper inlet temperature is T_{in} [K], and the stripper outlet temperature is T_{out} [K].

$$Q_H = W_S C_p (T_{out} - T_{in}) / W_{CO2} \quad (4)$$

Figure 12 shows the breakdown of regeneration heat of AMP 40 wt%+MAPA 5 wt% in comparison with the previous results of AMP 50 wt%+PZ 5 wt%. The sensible heat of this test was 0.48 GJ/ton-CO_2, which corresponded to a decrease of 11–39% against the result of AMP 50 wt%+PZ 5 wt% under the same condition.

The CO_2 recovery rate was obtained by the supplied CO_2 gas flow rate and CO_2 captured in the absorber. The supplied CO_2 gas flow rate was 2.2 L/min, which corresponds to 240 g/h. Since CO_2 captured in the absorber was 217 g/h, the CO_2 recovery rate was 90%.

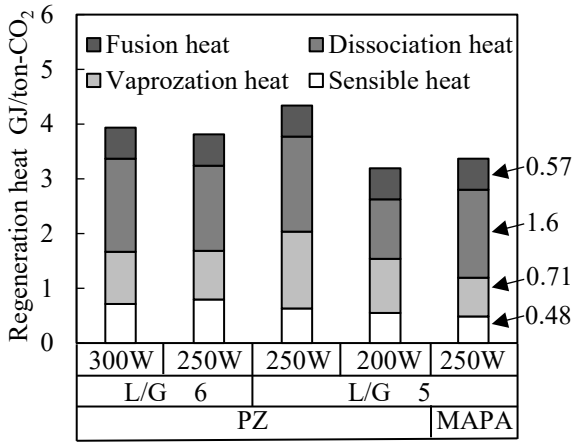

Figure 12. Regeneration heat of AMP 50wt%+PZ 5wt% and AMP 40wt%+MAPA 5wt%

5 Conclusion

This study aimed to improve the CO_2 recovery rate via selecting new promoter and modification of absorber configuration and cooling condition in the phase separation process using high-concentration AMP. The reaction rate test showed higher CO_2 absorption rate by adding MAPA than that by adding PZ, as such, AMP/MAPA solution was selected as a new solution. Simulation of the absorber column indicated that the highest CO_2 recovery rate and precipitate quantity were obtained by sending semi-lean liquid to central portion of the absorber column. In CO_2 capture and recovery tests with the new solution and the mid-column injection of semi-lean liquid, CO_2 recovery rate reached to 90% and the sensible heat was reduced to 0.48 GJ/ton-CO_2.

References

Bernhardsen, I. and H. Knuutila; “A Review of Potential Amine Solvents for CO_2 Absorption Process: Absorption

Capacity, Cyclic Capacity and pKa," *International Journal of Greenhouse Gas Control,* **61**, 27–48 (2017a)

Bernhardsen, I., I. Krokvik, K. Jens, and H. Knuutila; "Performance of MAPA Promoted Tertiary Amine Systems for CO_2 Absorption: Influence of Alkyl Chain Length and Hydroxyl Group," *Energy Procedia*, **114**, 1682–1688 (2017b)

Dash, S., A. Samanta, and S. Bandyopadhyay; "(Vapour + liquid) Equilibria (VLE) of CO2 in Aqueous Solutions of 2-amino-2-methyl-1-propanol: New Data and Modelling Using eNTRL-equation," *The Journal of Chemical Thermodynamics,* **43**, 1278–1285 (2011)

Inoue, S., T. Itakura, T. Nakagaki, T. Furukawa, H. Sato, and Y. Yamanaka; "Experimental Study on CO_2 Solubility in Aqueous Piperazine/alkanolamines Solutions at Stripper Conditions," *Energy Procedia*, **37**, 1751–1759 (2013)

IPCC, 2018: Global Warming of 1.5°C.An IPCC Special Report on the Impacts of Global Warming of 1.5°C above Pre-industrial Levels and Related Global Greenhouse Gas Emission Pathways, in the Context of Strengthening the Global Response to the Threat of Climate Change, Sustainable Development, and Efforts To Eradicate Poverty, V. Masson-Delmotte, P. Zhai, H.-O. Pörtner, D. Roberts, J. Skea, P. R. Shukla, A. Pirani, W. Moufouma-Okia, C. Péan, R. Pidcock, S. Connors, J. B. R. Matthews, Y. Chen, X. Zhou, M. I. Gomis, E. Lonnoy, T. Maycock, M. Tignor, and T. Waterfield eds (2018) in press

Kobari, M.; "New Interpreting Crystallization Process and Solvent-mediated Polymorphic Transformation," *JGC Technical Journal*, **6**, No.4 (2014)

Nakagaki, T., S. Inoue, S. Sato, Y. Furukawa, and H. Sato; "Evaluation of Energy in Precipitating 2-Amino-2-methyl-1-propanol Carbonate Solvent Process for CO_2 Capture," Post-Combustion Capture Conference 2, 1a-2, Bergen, Norway (2013)

Nakagaki, T., S. Sato, H. Sato, and Y. Yamanaka; "Experimental Measurement of Regeneration Energy in CO_2 Capture System Applying Phase Separation Process using high-concentration 2-Amino-2-methyl-1-propanol," Post-Combustion Capture Conference 3, 1B-2, Regina, Canada (2015)

Ogiyama, N., T. Hiro, H. Sato, J. Arakawa, and T. Nakagaki; "Stable Operation by Bench-scale CO_2 Capture Apparatus Applying Phase Separation Process," The Society of Chemical Engineers, Japan 49th Autumn Meeting., CA214, Nagoya, Japan (2017)

UNFCCC, V.; "Adoption of the Paris agreement." I: Proposal by the President (Draft Decision), United Nations Office, Geneva (Switzerland), (s 32). (2015)

Teranishi, H., H. Sato, J. Arakawa, Y. Yamanaka, and T. Nakagaki; "Modelling the Improvement of CO_2 Capture Efficiency by Way of a Novel CO_2-AMP Crystallization and Precipitation Process Using Aspen Plus," The Society of Chemical Engineers, Japan 48th Autumn Meeting., U121, Tokushima, Japan (2016)

Ying, J., S. Raets, and D. Eimer; "The Activator Mechanism of Piperazine in Aqueous Methyldiethanolamine Solutions." *Energy Procedia,* **114**, 2078–2087 (2017)

Zhang, R., X. Luo, Q. Yang, H. Yu, G. Puxty, and Z. Liang; "Analysis for the Speciation in CO_2 Loaded Aqueous MEDA and MAPA Solution Using ^{13}C NMR Technology," *International Journal of Greenhouse Gas Control*, **71**, 1–8 (2018)